View metadata, citation and similar papers at core.ac.uk

brought to you by CORE

provided by Aaltodoc Publication Archive

This is an electronic reprint of the original article.
This reprint may differ from the original in pagination and typographic detail.

Author(s): Lehtola, V. & Punkkinen, O. & Ala-Nissilä, Tapio

Title: Polymer scaling and dynamics in steady-state sedimentation at infinite Péclet number

Year: 2007

Version: Final published version

Please cite the original version:

Lehtola, V. & Punkkinen, O. & Ala-Nissilä, Tapio. 2007. Polymer scaling and dynamics in steady-state sedimentation at infinite Péclet number. Physical Review E. Volume 76, Issue 5. P. 051802/1-7. ISSN 1539-3755 (printed). DOI: 10.1103/physreve.76.051802.

Rights: © 2007 American Physical Society (APS). http://www.aps.org

All material supplied via Aaltodoc is protected by copyright and other intellectual property rights, and duplication or sale of all or part of any of the repository collections is not permitted, except that material may be duplicated by you for your research use or educational purposes in electronic or print form. You must obtain permission for any other use. Electronic or print copies may not be offered, whether for sale or otherwise to anyone who is not an authorised user.

Polymer scaling and dynamics in steady-state sedimentation at infinite Péclet number

V. Lehtola,[1] O. Punkkinen,[1] and T. Ala-Nissila[1,2,*]
[1]*Laboratory of Physics, Helsinki University of Technology, P.O. Box 1100, FIN-02015 TKK, Finland*
[2]*Department of Physics, Brown University, Providence, Rhode Island 02912-1843, USA*
(Received 9 March 2007; published 8 November 2007)

We consider the static and dynamical behavior of a flexible polymer chain under steady-state sedimentation using analytic arguments and computer simulations. The model system comprises a single coarse-grained polymer chain of N segments, which resides in a Newtonian fluid as described by the Navier-Stokes equations. The chain is driven into nonequilibrium steady state by gravity acting on each segment. The equations of motion for the segments and the Navier-Stokes equations are solved simultaneously using an immersed boundary method, where thermal fluctuations are neglected. To characterize the chain conformation, we consider its radius of gyration $R_G(N)$. We find that the presence of gravity explicitly breaks the spatial symmetry leading to anisotropic scaling of the components of R_G with N along the direction of gravity $R_{G,\parallel}$ and perpendicular to it $R_{G,\perp}$, respectively. We numerically estimate the corresponding anisotropic scaling exponents $\nu_\parallel \approx 0.79$ and $\nu_\perp \approx 0.45$, which differ significantly from the equilibrium scaling exponent $\nu_e = 0.588$ in three dimensions. This indicates that on the average, the chain becomes elongated along the sedimentation direction for large enough N. We present a generalization of the Flory scaling argument, which is in good agreement with the numerical results. It also reveals an explicit dependence of the scaling exponents on the Reynolds number. To study the dynamics of the chain, we compute its effective diffusion coefficient $D(N)$, which does not contain Brownian motion. For the range of values of N used here, we find that both the parallel and perpendicular components of D *increase* with the chain length N, in contrast to the case of thermal diffusion in equilibrium. This is caused by the fluid-driven fluctuations in the internal configuration of the polymer that are magnified as polymer size becomes larger.

DOI: 10.1103/PhysRevE.76.051802 PACS number(s): 82.35.Lr, 47.57.Ng

I. INTRODUCTION

The rheological properties of polymer melts and solutions have been under intense study for many decades due to their non-Newtonian hydrodynamic behavior and important applications in materials processing [1]. Most recently, with the rapidly developing field of nanofluidics and microfluidics [2,3], and their important application in "lab-on-a-chip" based technologies, it has become crucial to understand the behavior of single (bio) molecules in restricted geometries, and under nonequilibrium conditions. Using modern fluorescence techniques, it is now possible to experimentally measure the transport of individual DNA fragments in nanofluidic and microfluidic channels [4]. In the case of shear flow, in particular, there exist numerous experimental [5–11] and theoretical [12,13] studies of single-chain dynamics.

However, in microchannels the polymer transport is typically driven by an external force or by a pressure-driven flow [4,14]. In the special case where the external force is due to gravity, the problem of chain transport through a Newtonian solvent fluid becomes a problem of *sedimentation* of the polymer chain [15]. In the dilute limit, the sedimentation of rigid bodies such as spheres and spheroids and rods is well understood. However, at finite volume fractions the dynamics of even simple spherical particles is highly nontrivial [16–19]. Moreover, it has been shown that inertial effects can play a very significant role in the orientational behavior of spheroids. This raises an interesting question regarding the sedimentation of flexible polymer chains. As a polymer chain is inherently a many-particle system with strong topological constraints (as determined by the connectivity and nonoverlap conditions for the monomers), it is expected that chain dynamics under steady-state flow is highly nontrivial, too.

In this paper, our aim is to quantitatively model the steady-state sedimentation of a single polymer chain in a good solvent. To this end, we consider a general coarse-grained model of a flexible polymer chain in a good solvent. The chain is dragged through the liquid by gravity. By using a recently developed immersed boundary method [16–19] we couple the motion of the chain to a Newtonian fluid as described by full Navier-Stokes equations with a finite Reynolds number Re in the noncolloidal limit, where there is no Brownian motion. We study the scaling of the radius of the gyration of the chain and its velocity fluctuations under steady state. Our numerical results demonstrate that the hydrodynamic coupling of the individual segments leads to static and dynamical scaling behavior of the chain. To theoretically explain these results, we consider a generalization of the Flory argument for the present case of steady-state sedimentation. In particular, this argument reveals an explicit dependence of the scaling on the effective Re of the chain thus highlighting the importance of inertial effects in gravity-driven microflows of polymers.

II. MODEL

The model system we consider in this work comprises a single polymer chain immersed in a good solvent. As we wish to keep the model as general as possible, we use the

*Author to whom correspondence should be addressed.

 ©2007 The American Physical Society

standard coarse-grained bead-spring model of polymers [20,21]. There is a repulsive Lennard-Jones type of pair potential $V_{\mathrm{LJ}}(r)$ between all beads to prevent overlap, and a finitely extensible nonlinear elastic (FENE) potential $V_{\mathrm{FENE}}(r)$ between adjacent beads [22]. They are given by

$$V_{\mathrm{LJ}}(r) = 4\epsilon\left(\frac{\sigma}{r}\right)^{12},$$

$$V_{\mathrm{FENE}}(r) = -0.5kR_0^2 \ln\left[1 - \left(\frac{r}{R_0}\right)^2\right], \tag{1}$$

where $k=30\epsilon/\sigma^2$, $R_0=1.5\sigma$, and $\sigma=2a$. The distance between particles r is the distance between their center-of-mass (c.m.) and a is the radius of the Kuhn segment. The parameters were set to $\epsilon=30$ and $a=1$ here. The gravitational constant is 3, and it is used in the Navier-Stokes solver explained in [23]. This results into one-particle Stokes velocity of 0.55.

The fluid phase in the system is treated as continuum in a periodic three-dimensional (3D) box by using the full Navier-Stokes equations with a finite Reynolds number Re. The Reynolds number is an estimate of the ratio between the inertial and viscous forces in the Navier-Stokes equation, and is given by

$$\mathrm{Re} = \frac{2UL\rho}{\eta}, \tag{2}$$

where U and L denote the typical velocity and length scales in the system, and η is the fluid viscosity. The factor of 2 is included for convenience. In the present work, we set the single-particle Reynolds number Re=0.25 for most of the numerical work. If we neglect the inertial forces, we end up with the Stokes approximation Re=0, which is commonly used in analytic and numerical studies [15]. However, recent works have shown that inertial effects can play an important role when particle dynamics is considered under steady-state sedimentation [16–19].

In the numerical computation, we simultaneously solve for the discrete particle phase and the Navier-Stokes equations using a multigrid solver for the Navier-Stokes fluid [19,23]. The no-slip boundary condition between the fluid and the particles is implemented using the idea of the immersed boundary method first introduced by Fogelson and Peskin [24]. The method assumes that the fluid fills the whole volume of the system. This model has been tested extensively and used previously for studies of steady-state sedimentation of spherical particles and spheroids [16–19]. It should be noted that in the model the particles are non-Brownian, with an effectively infinite Péclet number Pe, which is the dimensionless measure of the relative importance of flow and thermal diffusion in the suspension

$$\mathrm{Pe} = \frac{UL}{D}, \tag{3}$$

where D is the thermal diffusivity. In the case of a sedimenting particle in a gravitational field one may assume that U equals the Stoke's velocity of a falling particle, in which case the Péclet number can be written as

$$\mathrm{Pe} = \frac{\Delta mgL}{k_BT}, \tag{4}$$

where g is the usual acceleration due to gravity, and Δm is the mass density between the sedimenting particle and the mass of an equal volume of fluid. Here we set the density difference between the particles and the fluid to be 1.5 times the density of the fluid. If we consider a suspension in water at room temperature ($T=293$ K), in which Pe=100, for example, the sedimenting particles (assumed to be spheres) would have a radius of about 1.6 μm and a mass of 2.5×10^{-14} kg in this non-Brownian limit.

III. RESULTS

A. Finite-size effects

The presence of long-range hydrodynamic interactions makes it crucially important to test the role of finite-size effects, which are important for sedimentation [18]. We have checked the finite-size effects by requiring that the distribution of the radius of gyration R_G [cf. Eq. (3)] and the average terminal velocity of the center of mass $\mathbf{v}_{\mathrm{lim}} \equiv \mathbf{v}_{\mathrm{c.m.}} - \delta\mathbf{v}_{\mathrm{c.m.}}$ must be unaffected by the change of the system size. We find that for a polymer of N beads, the grid size must be at least $2N\times2N\times6N$ grid points, where $6N$ is the system size in the direction parallel to gravity. Satisfying this requirement limits the systems we can presently study to a maximum chain length of $N=42$ due to computational demands. We have additionally checked that in our model the self-avoidance condition for the polymer chain is satisfied with the present choice of parameters.

B. Radius of gyration

Starting from an initial state with zero velocity, it takes the polymer chains typically less than about 1500 single-particle Stokes times to reach its steady-state distribution. In the steady state, we have determined the average radius of gyration from

$$R_G^2 = \frac{1}{N}\left\langle \sum_i^N (\bar{\mathbf{r}} - \mathbf{r}_i)^2 \right\rangle, \tag{5}$$

where i indexes the beads and $\bar{\mathbf{r}}=\Sigma_i^N\mathbf{r}_i/N$ is the location of the c.m. The angle brackets denote averaging over steady-state configurations. We have chosen the coordinate system such that the gravity force points toward the negative z axis. Thus, the z axis is the direction parallel to the flow ($\|$), and the xy plane is perpendicular ($\perp$) to it. This allows us to write

$$R_G^2 = R_{G,\|}^2 + R_{G,\perp}^2. \tag{6}$$

In Fig. 1 we show a time series of behavior of the two components of the radius of gyration for $N=32$. The steady state is characterized by large fluctuations in the size of the polymer, and the overall radius is larger perpendicular to the flow for this value of N. While the shape fluctuations appear rather chaotic (temporal Fourier analysis shows no peaks corresponding to periodic oscillations), it is interesting to

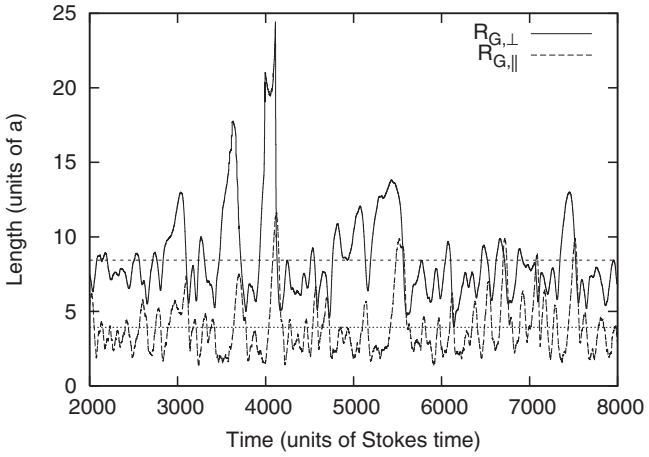

FIG. 1. Raw data for the components of the radius of gyration with $N=32$ in the steady state. The vertical lines indicate the average value of the respective component, calculated from the whole simulation data, of which only a small part is shown in the figure.

notice that the polymer seems to have two characteristic shapes, where the polymer is either extended along the flow (with large $R_{G,\parallel}$) or on the plane perpendicular to it (large $R_{G,\perp}$). The minima and maxima for these two components of R_G are temporally out of phase, as expected. In Fig. 2 we show snapshots of typical configurations corresponding to how a transition occurs between these two states. First, self-avoidance extends the polymer in the direction perpendicular to gravity. Then, the back-flow caused by the settling polymer creates a smaller pressure in the upward direction. As a consequence, the polymer is elongated in the positive z direction. The part that is left behind is pulled down by the spring forces, making the polymer collapse into a globule. Finally, the self-avoiding effects extend the chain in a perpendicular direction, and the polymer returns back to its original horizontally extended state.

We also note that the time-series data indicate a perfect correlation between the polymer's c.m. velocity and $R_{G,\perp}(t)$. This is in qualitative agreement with the Stokes friction formula that the limiting velocity should be inversely proportional to the component perpendicular to flow of the radius

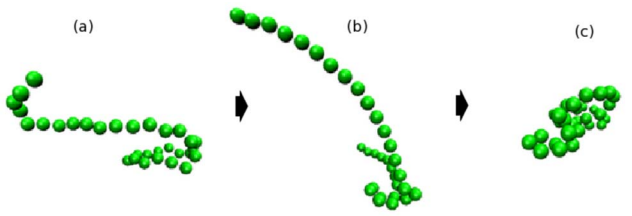

FIG. 2. (Color online) Snapshots of typical configurations of a settling polymer with $N=32$ in the steady state. The polymer is elongated in the horizontal direction (a). The loose end of the polymer is attracted by the smaller pressure caused by back-flow, and the polymer elongates in the vertical direction (b). The spring forces pull the part that is left behind, and the polymer collapses into a globular shape (c), which then expands due to self-avoidance leading back to a shape of the type in (a).

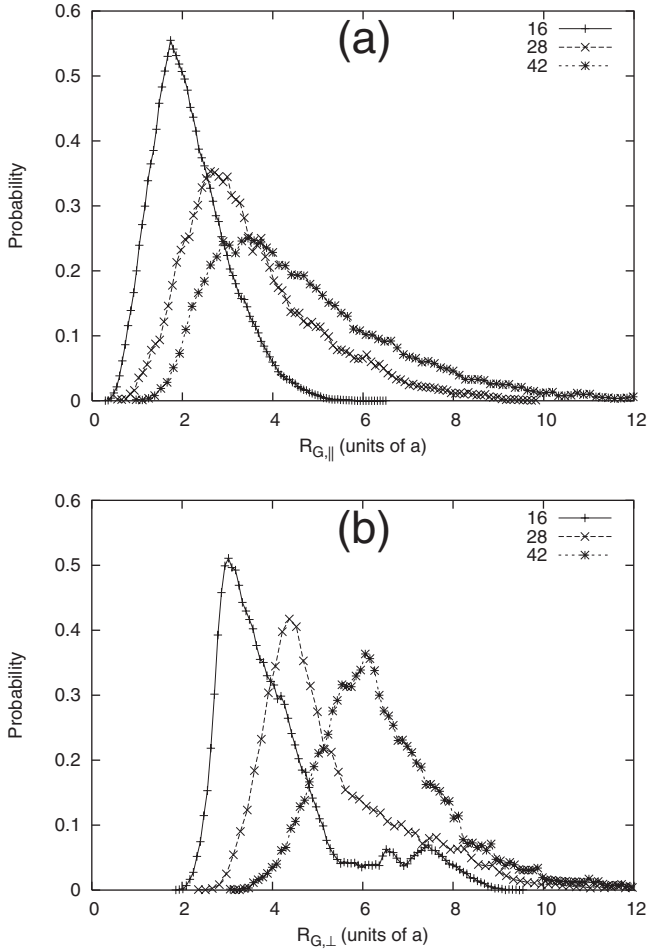

FIG. 3. The distributions of the two components of the radius of gyration: (a) in the direction parallel to gravity, and (b) in the direction perpendicular to gravity. The chain lengths are indicated in the figures.

of the object, namely $v_\parallel \propto 1/R_{G,\perp}$. However, quantitatively we find that $v_\parallel \propto N^{0.20\pm0.02}$, which is probably due to the increasing $\mathrm{Re}_{\mathrm{pl}}$ number of the polymer chain as a function of N, as will be discussed in the next section.

In Fig. 3 we show the actual distributions for $R_{G,\parallel}$ and $R_{G,\perp}$ for chains of length $N=16$, 28, and 32. These distributions are quantitatively different from the usual distribution of R_G in equilibrium. The spatial symmetry breaking induced by gravity is also clearly seen. In Fig. 4 we show the dependence of $R_{G,\parallel}$ and $R_{G,\perp}$ on N for $N=16$, 20, 24, 28, 32, and 42. In this range of N, we find that power-law scaling for both components of R_G is well satisfied, with

$$R_{G,\parallel} \propto N^{\nu_\parallel},$$

$$R_{G,\perp} \propto N^{\nu_\perp}, \tag{7}$$

where $\nu_\parallel=0.79\pm0.02$ and $\nu_\perp=0.45\pm0.01$. For comparison, we also show the scaling of the total radius of gyration $R_G \sim N^{\nu}$, with $\nu=0.50\pm0.01$. All of these values are clearly different from the 3D self-avoiding walk exponent in equilibrium, which is $\nu_e=0.588$ [20]. The larger scaling exponent of

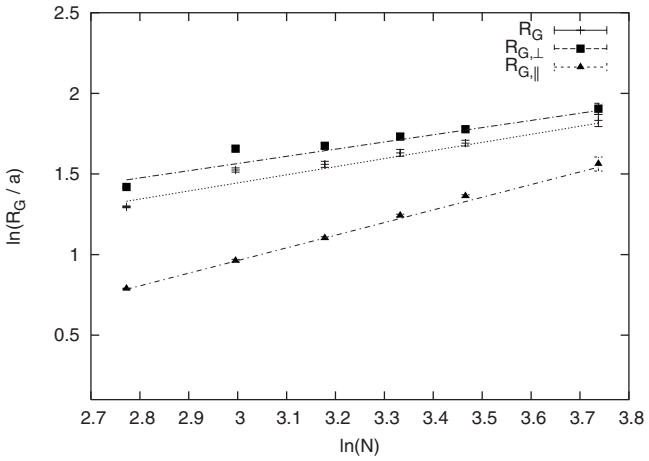

FIG. 4. Dependence of the total radius of gyration R_G and its parallel and perpendicular components on the chain length N, plotted on a log-log scale. The values of the scaling exponents are $\nu=0.50\pm0.07$, $\nu_{\parallel}=0.79\pm0.02$, and $\nu_{\perp}=0.45\pm0.01$. From these data we have extrapolated the critical value of N, where the parallel component of the radius of gyration exceeds the perpendicular component to be ≈ 120.

the parallel component indicates that the ratio $R_{G,\parallel}/R_{G,\perp}$ actually *grows* with increasing N, and thus the parallel component becomes eventually larger than the perpendicular one for long enough chains assuming that the present scaling holds for larger values of N as well. From our scaling data, we can extrapolate that this happens for $N \approx 120$ (see Fig. 4). This means that on the average long chains become extended along the direction of sedimentation, in qualitative agreement with a recent numerical study of polymer sedimentation with Re=0 [15].

C. Generalized Flory argument

For a polymer chain in thermal equilibrium, the classic Flory mean-field argument [20] gives a very good approximation of the true scaling exponent for $R_G(N)$. In order to explain the numerical scaling results in the preceding section, we present here a generalization of the Flory argument for the present case of a polymer chain in a steady-state flow. To this end, we construct an equilibrium free energy function for the polymer as a function of $R_G(N)$ following the approach of Flory, but adding a kinetic energy term [25]. This kinetic term describes the nonequilibrium behavior, and setting it to zero recovers the equilibrium scaling limit. Thus, the total energy of the polymer chain consists of the spring forces between the monomers, the self-avoidance and the kinetic energy contribution, and can be written as

$$E_{\text{total}} = \frac{1}{2}\frac{k}{N}R_G^2 + \frac{1}{2}\nu c^2 R_G^3 + \frac{1}{2}(m_0 N)\mathbf{v}_{\text{c.m.}}(R_G)^2, \qquad (8)$$

where N is the number of monomers, k is the spring constant between two monomers, m_0 is the mass of one monomer, and $c \simeq N/R_G^3$ is the concentration of monomers per volume. Furthermore, $\mathbf{v}_{\text{c.m.}}(R_G)$ is the velocity of the center of mass for a given configuration R_G.

We can further justify the inclusion of the kinetic energy term by the following argument. In the steady state, the c.m. of the polymer chain has reached its limiting (Stokes) velocity in the fluid $\mathbf{v}_s$. At the steady state the velocity field of the chain is coupled to its instantaneous configuration in a highly nontrivial way. Any modification in the internal configuration of chain automatically induces a change in the velocity field, and vice versa. As a consequence, the c.m. velocity of the chain also fluctuates. In the limit of Pe=∞, this is the only source of velocity fluctuations. If we assume that the velocity field adapts infinitely fast to configurational changes of the chain, we can say that $\mathbf{v}_{\text{c.m.}} \equiv \mathbf{v}_{\text{c.m.}}(R_G)$. This means that momentum transport of the fluid is much faster than the particle transport, i.e., the changes in the velocity field created by the falling polymer relax much faster than the changes in the internal configuration of the polymer. Thus, the chain has a quadratic kinetic energy term arising from these inertial fluctuations, given by the additional term proportional to $\mathbf{v}_{\text{c.m.}}^2$.

Next, we make the assumption that the c.m. velocity can be separated as $\mathbf{v}_{\text{c.m.}} = \mathbf{v}_{\text{lim}} + \delta\mathbf{v}_{\text{c.m.}}$, thus consisting of the driven constant velocity $\mathbf{v}_{\text{lim}} \equiv \langle \mathbf{v}_{\text{c.m.},\parallel} \rangle$ and of small fluctuations $\delta\mathbf{v}_{\text{c.m.}} \equiv \mathbf{v}_{\text{c.m.}} - \mathbf{v}_{\text{lim}}$. This can be justified by $|\mathbf{v}_{\text{lim}}| \gg |\delta\mathbf{v}_{\text{c.m.}}|$, i.e., the average limiting velocity is much larger than fluctuations in the c.m. velocity. The kinetic energy term can be then simplified by using the decomposition

$$\mathbf{v}_{\text{c.m.}}(R_G)^2 = \mathbf{v}_{\text{lim}}^2 + 2\mathbf{v}_{\text{lim}} \cdot \delta\mathbf{v}_{\text{c.m.}}(R_G) + [\delta\mathbf{v}_{\text{c.m.}}(R_G)]^2, \quad (9)$$

where $\mathbf{v}_{\text{lim}}$ is now independent of R_G. Furthermore, the numerical scaling results in the preceding section show that the scaling exponent of the parallel component of $R_G(N)$ is much larger than that of the perpendicular. In other words, the polymer is more stretched out in the parallel direction. Thus, to lowest order

$$V_p = R_G^3 \approx R_{G,\parallel} R_{G,\perp}^2, \qquad (10)$$

where V_p is the volume occupied by the polymer.

To estimate the fluctuating part of the velocity, we assume that the polymer internal motion happens slowly as compared to the external velocity, and thus we can use the Stokes approximation (Re=0) for the hydrodynamical tensor. The velocity induced velocity fluctuations are then given by the Zimm model [26] as $|\delta\mathbf{v}| \propto 1/R_G \simeq 1/R_{G,\parallel}$ in the limit where N is large.

Plugging in these approximations to Eq. (8), we obtain the following functional form for the free energy of the chain:

$$E_{\text{total}} \propto \frac{1}{2}\frac{k}{N}R_{G,\perp}^2 + R_{G,\parallel}^2 + \frac{1}{2}\nu\frac{N^2}{R_{G,\perp}^2 R_{G,\parallel}} + \frac{1}{2}(m_0 N)\left(\frac{|\mathbf{v}_{\text{lim}}|}{R_{G,\parallel}} + \frac{1}{R_{G,\parallel}^2}\right). \qquad (11)$$

Here we have discarded the quadratic term in $\mathbf{v}_{\text{lim}}$, being independent of R_G. The equilibrium is obtained by minimizing the free energy with respect to both $R_{G,\perp}$ and $R_{G,\parallel}$ separately,

TABLE I. Comparison between the numerically obtained scaling exponents and the theoretical predictions from the generalized Flory argument for low and high Re limits.

	Results	Theory ($\beta=1$)	Theory ($\beta=1/2$)
$\nu_\perp$	0.45±0.07	0.545	0.591
$\nu_\parallel$	0.79±0.02	0.818	0.636

$$\frac{\partial E_{\text{total}}}{\partial R_{G,\parallel}} = 0 \quad \text{and} \quad \frac{\partial E_{\text{total}}}{\partial R_{G,\perp}} = 0. \tag{12}$$

With some algebra we have the following results for the average components of R_G:

$$\langle R_{G,\parallel}\rangle \propto N^{2/3}|\mathbf{v}_{\text{lim}}|^{1/3}, \tag{13}$$

$$\langle R_{G,\perp}\rangle \propto N^{7/12}|\mathbf{v}_{\text{lim}}|^{-1/12}. \tag{14}$$

Equations (13) and (14) are the main results of this section. In the case of the polymer chain, we can estimate the dependence of the limiting velocity on R_G by assuming that it is determined simply by the average size of the polymer in the direction perpendicular to gravity. Then, using the Stokes formula $6\pi\eta R|\mathbf{v}_{\text{lim}}|=Mg$, M being the total mass of the polymer, we can deduce that

$$\mathbf{v}_{\text{lim}} \propto \frac{m_0 N}{\langle R_{G,\perp}\rangle}. \tag{15}$$

From this it follows that in the limit of low Re, the scaling of the components of the radius of gyration is given by $\langle R_{G,\perp}\rangle \propto N^{6/11} \simeq N^{0.545}$ and $\langle R_{G,\parallel}\rangle \propto N^{9/11} \simeq N^{0.818}$. These results are consistent with our previous assumption that $R_{G,\parallel} \gg R_{G,\perp}$ for large N.

The generalized Flory argument presented here can also be applied without invoking the Stokes formula for cases where Re is not small. Unfortunately, we are not aware of any exact results in this regime. However, as explained in detail in the Appendix, there exists an empirical high Re expansion formula for the limiting velocity, which is given by

$$\frac{Mg}{|\mathbf{v}_{\text{lim}}|} = 6\pi R_{G,\perp}\eta\left(1 + \frac{\text{Re}}{4(1+\sqrt{\text{Re}})} + 0.017\ \text{Re}\right), \tag{16}$$

which reduces to the Stokes equation when $\text{Re} \ll 1$. This can be written as

$$|\mathbf{v}_{\text{lim}}| \propto N^{\beta-\nu_\perp}, \tag{17}$$

where $\beta=1$ for $\text{Re} \ll 1$ and $\beta=1/2$ for $\text{Re} \gg 1$. Inserting this into Eq. (14), we obtain the general result that

$$\langle R_{G,\parallel}\rangle \propto N^{(15+12\beta)/33}, \tag{18}$$

$$\langle R_{G,\perp}\rangle \propto N^{(7-\beta)/11}. \tag{19}$$

In Table I, we present a comparison between the numerically and theoretically obtained scaling exponents for low and high Re.

We note that the empirical formula in Eq. (A4) is valid only for $\text{Re} < 2\times 10^5$, after which the flow becomes turbulent. It should be noted that below that threshold, but with high Re, the N dependence of the terminal velocity is of the form $|\mathbf{v}_{\text{lim}}| \propto N^{0.05}$ using our numerical result for $\nu_\perp$. In other words, in this limit the N dependence of $\mathbf{v}_{\text{lim}}$ becomes very weak.

D. Velocity fluctuations and effective diffusion

A direct consequence of the random velocity fluctuations around the steady-state limit is that in analogy to thermal systems, such fluctuations lead to the existence of finite transport coefficients [16–19]. In particular, using the Green-Kubo response function formalism [27,28] the effective diffusion coefficient for the c.m. of the polymer chain can be defined by

$$D = \frac{1}{d}\lim_{T\to\infty}\int_0^T dt\langle \delta\mathbf{v}_{\text{c.m.}}(t)\cdot\delta\mathbf{v}_{\text{c.m.}}(0)\rangle. \tag{20}$$

Here the velocity fluctuation $\delta\mathbf{v}_{\text{c.m.}} \equiv \mathbf{v}_{\text{c.m.}} - \langle\mathbf{v}_{\text{c.m.}}\rangle$ is as defined in the preceding section, and $d=3$ is the dimension of the embedding space. In thermal equilibrium, the equilibrium diffusion coefficient of a polymer chain in a good solvent is known to scale as [20]

$$D \propto N^{-\nu_D}, \tag{21}$$

where $\nu_D=1$ for the Rouse model, and $\nu_D=\nu_e$ for the Zimm model. In the presence of the symmetry breaking gravitational field, we expect this scaling law to generalize to two independent relations as

$$D \propto N^{-\nu_{D,\parallel}},$$

$$D_\perp \propto N^{-\nu_{D,\perp}}. \tag{22}$$

To compute D here, we have calculated the velocity fluctuation correlation functions in the steady-state regime, and used the memory expansion method of Ref. [29]. Due to large fluctuations in the data, we have been able to consider chains of length $N=16$, 20, 28, and 32 only. In Fig. 5 we show the scaling of the components of D for this range of chain lengths. The surprising result here is that we find that for this range of values of N both diffusion coefficients actually *increase* with increasing N, in contrast to the thermal case. Best fit to the data gives $\nu_{D,\perp}=-0.22\pm0.11$ and $\nu_{D,\parallel}=-1.0\pm0.2$. In the present case this behavior can be qualitatively explained by the fact that in the limit of $\text{Pe}=\infty$, the increasing size of the polymer increases the terminal velocity of the chain. Numerically, we find that $|\mathbf{v}_{\text{lim}}| \propto N^{0.2}$ for the present range of values of N. Due to the fact that deterministic velocity fluctuations are proportional to the limiting velocity of the sedimenting polymer, they are also amplified as the size of the polymer increases. Furthermore, Eq. (20) suggests, that $D \propto \mathbf{v}_{\text{lim}}^2$, thus implicating a positive scaling exponent ν_D for D. However, in order to quantitatively explain the asymmetry between $\nu_{D,\parallel}$ and $\nu_{D,\perp}$, a more refined theory is needed [30]. In particular, it is clear that D depends not

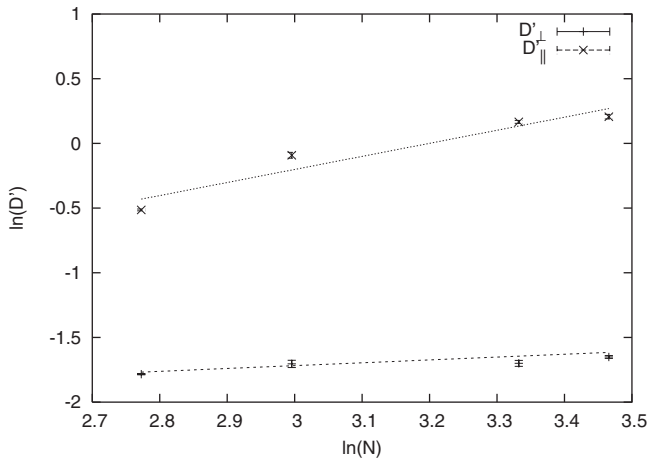

FIG. 5. The scaling of $D'_{\perp}=D_{\perp}\tau/a^2$ and $D'_{\parallel}=D_{\parallel}\tau/a^2$ vs chain length N. The measured scaling exponents are $\nu_{D,\perp}=-0.22\pm0.11$ and $\nu_{D,\parallel}=-1.0\pm0.2$. See text for details.

only on the overall settling velocity of the polymer, but also on the morphological fluctuations of the chain.

IV. SUMMARY AND CONCLUSIONS

In this work we have examined the behavior of a coarse-grained polymer chain in steady-state sedimentation. The Navier-Stokes fluid treated as a continuum has a finite one-particle Reynolds number (Re=0.25), and thus our model properly includes inertial effects. The nonequilibrium conditions dominate over thermal diffusion here. Under these conditions the chain reaches a steady state, and it continues to fluctuate irregularly through a series of configurations which include vertical and horizontal straightening and collapsing back to a globule. The settling velocity for the center of mass is found to have a strong correlation with the component of the radius of gyration perpendicular to the flow, in qualitative agreement with the Stokes result for particle settling velocity. The scaling exponents for the components of the radius of gyration $R_{G,\perp}$ and $R_{G,\parallel}$ are determined to be $\nu_{\parallel}=0.785\pm0.02$ and $\nu_{\perp}=0.446\pm0.068$, respectively, which are markedly different from the equilibrium results in 3D. To explain these results, we have developed a generalization of the Flory scaling argument for the present case. It predicts that the inertial forces induced by the nonequilibrium flow alter the configuration probabilities radically. In particular, there is explicit dependence of the values of the exponents on Re. While it is difficult to quantitatively compare the theoretical prediction with numerical results, the overall agreement is encouragingly good, as can be seen in Table I.

It is interesting to compare the chaotic shape fluctuations observed here to a recent study of polymer sedimentation in the limit Re=0 [15]. In this case, for long polymers and large driving (large Péclet number) force, chainlike polymers assume a stable, elongated configuration due to an effective stretching force on the chain. Our results indicate that such a configuration becomes unstable against hydrodynamic fluctuations for Re>0, at least for large Pe. Further systematic studies of this transition would be of great interest.

Finally, we have also considered velocity fluctuations and the corresponding effective c.m. diffusion coefficient of the chain in steady state. Chain lengths of $N\in[16,20,28,32]$ were used for the scaling of D. Due to symmetry breaking, the scaling is anisotropic. The unexpected result here is that for the present range of values of N, we actually find that both the parallel and perpendicular components of D *increase* with increasing N, and the corresponding exponents are given by $\nu_{D,\parallel}=-1.0\pm0.2$ and $\nu_{D,\perp}=-0.22\pm0.11$. This is an unusual result, since for the Rouse model $\nu_D=1$ and for the Zimm model $\nu_D=\nu$. However, it should be kept in mind that in our model there is no thermal component in the velocity fluctuations. The gravitational force acting on the polymer increases with its mass, leading to greatly amplified velocity fluctuations with N, in part through the increasing settling velocity of the chain. It would be of interest to consider the colloidal limit of steady-state sedimentation of polymer chains by adding the thermal motion to the system. This could be possible by using methods such as the lattice-Boltzmann technique [31] or the stochastic rotation-collision dynamics [32]. Work in this direction is in progress.

ACKNOWLEDGMENTS

The authors wish to thank Colin Denniston, Mikko Karttunen, Ilpo Vattulainen, and See Chen Ying for useful discussions. This work has been supported in part by the Academy of Finland through its Center of Excellence Program COMP, and the TransPoly consortium grant [to one of the authors (T.A-N.)]. One of the authors (O.P.) wishes to thank the Finnish Cultural foundation for support.

APPENDIX: EXTENSION TO HIGH REYNOLDS NUMBERS

The one-particle Re number for our model has a fixed value of Re=0.25. The polymer chain is described by its proper Reynolds number $\mathrm{Re}_{\mathrm{pl}}$, which can be written as

$$\mathrm{Re}_{\mathrm{pl}} \equiv \frac{2\rho|\mathbf{v}_{\mathrm{lim}}|R_{G,\perp}}{\eta}, \tag{A1}$$

where $\mathbf{v}_{\mathrm{lim}}$ is the averaged steady-state settling velocity of the center of mass. The factor of 2 is included for convenience. For an immersed sphere the drag coefficient C_D is given by [33]

$$C_D \equiv \frac{2F}{\rho\mathbf{v}_{\mathrm{lim}}^2\pi R_{G,\perp}^2}, \tag{A2}$$

and it remains nearly constant at high Reynolds numbers (up to about 2×10^5). The external force $F=Mg=Nm_0g$ increases as a function of the chain length N. With the help of Eqs. (A1) and (A2) we define the friction coefficient

$$\mu \equiv \frac{Mg}{|\mathbf{v}_{\mathrm{lim}}|} = \left(\frac{1}{4}\pi R_{G,\perp}\eta\right)\mathrm{Re}_{\mathrm{pl}}\, C_D, \tag{A3}$$

where the drag coefficient C_D is written as [33] $C_D=24/\mathrm{Re}+6/(1+\sqrt{\mathrm{Re}})+0.4$.

Using the empirical formula for C_D, Eq. (A3) becomes

$$\frac{Mg}{|\mathbf{v}_{\mathrm{lim}}|} = 6\pi R_{G,\perp}\eta\left(1 + \frac{\mathrm{Re}_{\mathrm{pl}}}{4(1+\sqrt{\mathrm{Re}_{\mathrm{pl}}})} + 0.017\ \mathrm{Re}_{\mathrm{pl}}\right). \tag{A4}$$

At the limit $\mathrm{Re}_{\mathrm{pl}} \to 0$, this reduces to the Stokes equation. For $\mathrm{Re}_{\mathrm{pl}} \gg 1$, the last term becomes dominant. We have the following proportionalities:

$$|\mathbf{v}_{\mathrm{lim}}| \propto N^{1-\nu_\perp}, \quad \mathrm{Re}_{\mathrm{pl}} \ll 1,$$

$$|\mathbf{v}_{\mathrm{lim}}| \propto N^{2/3-\nu_\perp} \quad \text{(middle term only)},$$

$$|\mathbf{v}_{\mathrm{lim}}| \propto N^{1/2-\nu_\perp}, \quad \mathrm{Re}_{\mathrm{pl}} \gg 1.$$

All of these share the common form of

$$|\mathbf{v}_{\mathrm{lim}}| \propto N^{\beta-\nu_\perp}, \tag{A5}$$

where β is a constant with a value from 1/2 to 1. The Reynolds number of a polymer $\mathrm{Re}_{\mathrm{pl}}$ is dependent on the chain length and the settling velocity, and it grows as the chain gets longer (and heavier) or the polymer experiences a faster flow. The prediction is that for large $\mathrm{Re}_{\mathrm{pl}}$ the settling velocity becomes nearly independent of the chain length, which is consistent with our result $|\mathbf{v}_{\mathrm{lim}}| \propto N^{0.05}$.

[1] R. B. Bird, R. C. Armstrong, and O. Hassager, *Dynamics of Polymeric Liquids* (Wiley-Interscience, New York, 2001), Vol. 1.

[2] N. T. Nguyen and S. T. Wereley, *Fundamentals and Applications of Microfluidics*, 2nd ed. (Artech House, Boston, 2006).

[3] T. M. Squires and S. R. Quake, Rev. Mod. Phys. **77**, 977 (2005).

[4] D. Stein, F. H. J. Van Der Heyden, W. J. A. Koopman, and C. Dekker, Proc. Natl. Acad. Sci. U.S.A. **103**, 15853 (2006).

[5] T. T. Perkins, D. E. Smith, and S. Chu, Science **276**, 2016 (1997).

[6] D. E. Smith, H. P. Babcock, and S. Chu, Science **283**, 1724 (1999).

[7] P. LeDuc, C. Haber, G. Bao, and D. Wirtz, Nature (London) **399**, 564 (1999).

[8] P. S. Doyle, B. Ladoux, and J.-L. Viovy, Phys. Rev. Lett. **84**, 4769 (2000).

[9] R. E. Teixeira, H. P. Babcock, E. S. G. Shaqfeh, and S. Chu, Macromolecules **38**, 581 (2005).

[10] S. Gerashchenko and V. Steinberg, Phys. Rev. Lett. **96**, 038304 (2006).

[11] C. M. Schroeder, R. E. Teixeira, E. S. G. Shaqfeh, and S. Chu, Phys. Rev. Lett. **95**, 018301 (2005).

[12] R. G. Winkler, Phys. Rev. Lett. **97**, 128301 (2006).

[13] V. Symeonidis, G. E. Karniadakis, and B. Caswell, Phys. Rev. Lett. **95**, 076001 (2005).

[14] O. B. Usta, J. E. Butler, and A. J. C. Ladd, Phys. Rev. Lett. **98**, 098301 (2007).

[15] X. Schlagberger and R. R. Netz, Phys. Rev. Lett. **98**, 128301 (2007).

[16] E. Kuusela, J. M. Lahtinen, and T. Ala-Nissila, Europhys. Lett. **65**, 13 (2004).

[17] E. Kuusela, J. M. Lahtinen, and T. Ala-Nissila, Phys. Rev. Lett. **90**, 094502 (2003).

[18] E. Kuusela, J. M. Lahtinen, and T. Ala-Nissila, Phys. Rev. E **69**, 066310 (2004).

[19] E. Kuusela, *Steady-State Sedimentation of Non-Brownian Particles with Finite Reynolds Number* (Otamedia Oy, Espoo, 2005).

[20] M. Doi and S. F. Edwards, *The Theory of Polymer Dynamics* (Oxford Science, Oxford, 1986).

[21] M. Kroger, Phys. Rep. **390**, 453 (2004).

[22] R. B. Bird, C. F. Curtiss, R. C. Armstrong, and O. Hassager, *Dynamics of Polymetric Fluids*, 2nd ed. (Wiley, New York, 1987), Vol. 2.

[23] E. Kuusela, K. Hofler, and S. Schwarzer, J. Eng. Math. **41**, 221 (2001).

[24] A. L. Fogelson and C. S. Peskin, J. Comput. Phys. **79**, 50 (1988).

[25] O. Punkkinen (unpublished).

[26] B. H. Zimm, J. Chem. Phys. **24**, 269 (1956).

[27] R. Kubo, J. Phys. Soc. Jpn. **12**, 570 (1957).

[28] R. Gomer, Rep. Prog. Phys. **53**, 917 (1990).

[29] S. C. Ying, I. Vattulainen, J. Merikoski, T. Hjelt, and T. Ala-Nissila, Phys. Rev. B **58**, 2170 (1998).

[30] O. Punkkinen, E. Falck, and I. Vattulainen, J. Chem. Phys. **122**, 094904 (2005).

[31] R. Kapral, A. Lawniczak, and P. Masiar, Phys. Rev. Lett. **66**, 2539 (1991).

[32] T. Ihle and D. M. Kroll, Phys. Rev. E **67**, 066705 (2003).

[33] F. M. White, *Viscous Fluid Flow* (McGraw-Hill, Singapore, 1991).